Facile synthesis of hollow nano-spheres and hemispheres of cobalt by polyol reduction

2010 Nanotechnology 21 375602

(http://iopscience.iop.org/0957-4484/21/37/375602)

Nanotechnology **21** (2010) 375602 (5pp) doi:10.1088/0957-4484/21/37/375602

Facile synthesis of hollow nano-spheres and hemispheres of cobalt by polyol reduction

Haitao Yang[1], **Chengmin Shen, Ningning Song, Yumei Wang, Tianzhong Yang, Hongjun Gao and Zhaohua Cheng**

Beijing National Laboratory for Condensed Matter Physics, Institute of Physics, Chinese Academy of Sciences, Beijing 100190, People's Republic of China

E-mail: htyang@aphy.iphy.ac.cn

Received 19 June 2010, in final form 29 July 2010
Published 17 August 2010
Online at stacks.iop.org/Nano/21/375602

Abstract

The hydrophilic hollow nano-spheres and hemispheres of Co are synthesized via ethylene glycol reduction of cobalt acetate in the presence of PVP and Pd nano-particle seeds. The dimensions of the hollow core can be tuned from 100 to 300 nm by controlling the amount of Pd nano-particle seeds. The morphology of the hollow materials strongly depends on the molar ratio of the amide unit in PVP over Co and the M_w of PVP. The hollow structure is formed when the ratio falls in the range 1–1.5 and the M_w is over 40 000. Based on the experimental data, a possible formation mechanism of Co hollow spheres is proposed.

S Online supplementary data available from stacks.iop.org/Nano/21/375602/mmedia

1. Introduction

Materials containing nano-scale pores have attracted great interest due to their roles as nano-capturers, nano-reactors and nano-channels. Such porous structures have less density and a much larger surface to volume ratio than their solid materials counterparts, and are potential candidates for applications in catalysis, optics and storage/separation devices [1–3]. The common procedures for making porous materials involve the applications of various colloidal templates [4–8]. Coating these templates with a variety of inorganic and organic species, followed by either calcinations or chemical etching, leads to porous materials with well-controlled pore dimensions. Alternatively, the porous structures can be made from the synergistic interface chemistry of inorganic and organic species [9–11], de-alloying of certain binary alloy systems [12, 13], or through the nano-scale Kirkendall effect [14], in which the outward flow of an element from a nano-sphere core results in a vacant core and a solid shell. The syntheses have yielded various polymeric, oxide, metal salt and metallic Au porous structures with interesting optical and chemical properties. Compared to these nonmagnetic porous systems, transition metal based magnetic porous structures have rarely been studied thus far [15, 16]. With characteristic pore features and magnetic maneuverability, such magnetic porous structures could serve as nano-reactors for catalysis, or as nano-capturers for magnetic-based separation and delivery tools.

Here we report the facile synthesis of hydrophilic hollow Co nano-spheres and hemispheres by polyol reduction of cobalt acetate, $Co(CH_3COO)_2$, in the presence of polyvinylpyrrolidone (PVP) and Pd nano-particle seeds. Polyol reduction has been used for the synthesis of various late transition metal nano-materials [17, 18]. Ethylene glycol (EG) is a common polyol used for the reduction reaction although other polyalcohols can also be used. PVP has been known for its protection of transition metal nano-particles due to the presence of the repeated amide (–N–CO–) group within its polymeric chain. Recently, Xia's group reported that during polyol reduction of gold/silver salt, PVP could be used to regulate the growth of Au/Ag nano-crystals on certain crystal faces, leading to well-controlled Au/Ag nano-boxes/nano-cubes or even nano-wires (upon the introduction of Pt seeds) [19, 20]. Using Pd nano-particles as seeds and EG reduction of cobalt acetate in the presence of PVP, we found that magnetic hollow structures of Co spheres and hemispheres were readily formed. The diameter of the hollow core was controlled by the amount of Pd nano-particle seeds

[1] Author to whom any correspondence should be addressed.

and was tunable from 100 to 300 nm with a corresponding shell thickness from 20 to 40 nm.

2. Experimental details

2.1. Synthesis of the nano-scale hollow Co

Anhydrous ethylene glycol (EG, 99.8%), palladium chloride ($PdCl_2$, 99.99%), cobalt acetate tetrahydrate ($Co(CH_3COO)_2 \cdot 4H_2O$, 99+%), polyvinylpyrrolidone (PVP), and acetone (HPLC grade) were purchased from Acros Chemicals and were used without further purification. Cobalt spheres and hemispheres were synthesized by reducing $Co(CH_3COO)_2$ with EG in the presence of Pd seeds and PVP, in a typical synthesis as follows: 30 ml of EG was loaded in a 100 ml three-neck-flask and was heated to ∼195 °C using an oil-bath under Ar. In two other separate conical flasks, 0.125 g $Co(CH_3COO)_2 \cdot 4H_2O$ and 0.088 g PVP were respectively dissolved in 3 ml EG. The concentrations of $Co(CH_3COO)_2$/EG and PVP/EG were 0.5 mmol and 0.75 mmol, respectively. When the reaction (EG) solution was heated to 195 °C, 0.5 ml of the EG solution of $PdCl_2$ (1.5×10^{-3} M) was injected into the reaction solution and immediately was reduced by EG to form black Pd nano-particles. After 1 min, 3 ml $Co(CH_3COO)_2$/EG (0.5 mmol) and 3 ml PVP/EG (0.75 mmol) solution were transferred using two separate syringes and were simultaneously added dropwise into the above hot solution over a period of 6 min. Then this reaction mixture was heated at 195 °C for another 120 min until the color of the solution changed to gray. The solution was cooled down to room temperature by removing the heat source. The mixture was centrifuged (500 rpm for 1 min) to remove any remaining unsolved precipitation, and the supernatant was precipitated by adding acetone. The black precipitate was collected using an NdFeB permanent magnet and washed with ethanol and acetone to remove excessive EG and PVP, then redispersed into deionized water. The yield was 35% (based on Co).

2.2. The sonication preparation of Co hemispheres

A 20ml volume of the Co hollow spheres aqueous solution was added into a flask. Then this flask was put into high power ultrasonicator (Power 200 W) and dispersed for 30 min. The sample was dropped onto the Si substrate for SEM analysis.

2.3. Hollow cobalt spheres characterization

Scanning electron microscopic (SEM) measurements were carried out with a field emission microscopic (FEI Corp. XL-SFEG) at an acceleration voltage of 20 kV. Transmission electron microscopy (TEM) images were obtained on a Philips CM200FEG operating at 160 kV and a Hitachi 9000 operating at 300 kV. The SEM samples were formed by dropping small droplets of the diluents onto silicon substrates. The TEM samples were formed by dropping one droplet of the diluents onto amorphous-carbon-coated copper grids. All the SEM and TEM samples were allowed to dry at room temperature. The elemental composition of the nano-crystals was obtained by inductively coupled plasma-atomic emission spectroscopy (ICP-AES). For these measurements, hollow Co nano-spheres were thoroughly washed to remove most of the organic ligands and subsequently dissolved in a standard HCl solution. Magnetic measurement was conducted in a physical properties measurement system (PPMS) 6000 at 300 and 10 K. The calculation of the saturation moment of Co hollow materials was performed using the mass of Co in PVP-coated Co hollow spheres based on ICP-AES analysis.

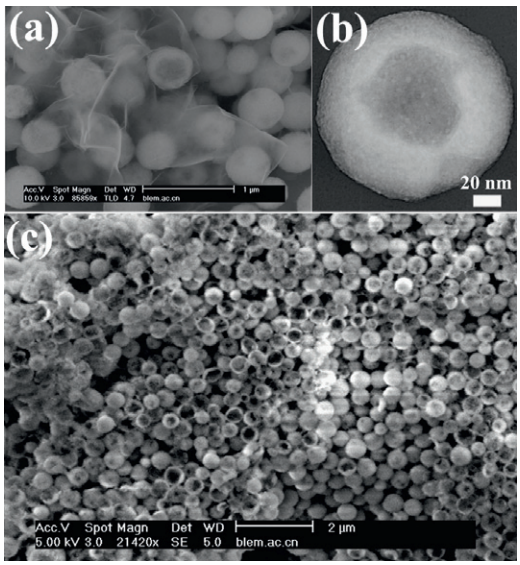

Figure 1. (a) SEM image of the hollow Co nano-spheres/hemispheres in the presence of excess PVP. (b) SEM image of the hollow Co obtained after a 2 min sonication. (c) TEM image of one hollow Co sphere with a hollow core at around 200 nm and shell around 45 nm.

3. Results and discussion

Figure 1 shows the electron microscopic images of the hollow Co spheres/hemispheres. Figure 1(a) is the SEM image of the hollow Co with the presence of an excess of PVP. After an acetone wash and a 2 min sonication, hollow hemispheres are more readily visible as shown in figure 1(b). The IMAGEJ 1.3.2J software was used to determine the average particle size and the size distribution by analyzing about 200 particles located in the selected rectangular area. Particles were identified by the contrast between particle and background, and their edges were outlined. The particle size was determined as the average of its major and minor axes. From the particle size distribution histogram, the average size of 233 nm and the relative size distribution of nearly 10% were obtained[2]. Figure 1(c) is a higher resolution TEM image of a hollow Co. It shows a cobalt shell thickness of around 45 nm. The image further reveals that the shell is not single crystalline Co but a system of smaller Co cluster aggregates. It is difficult to observe the clear lattice image of smaller aggregated Co clusters due to the strong interference of the PVP. However, from the analysis of the Williamson–Hall plot, we can gain

[2] See the supporting information available at stacks.iop.org/Nano/21/375602/mmedia.

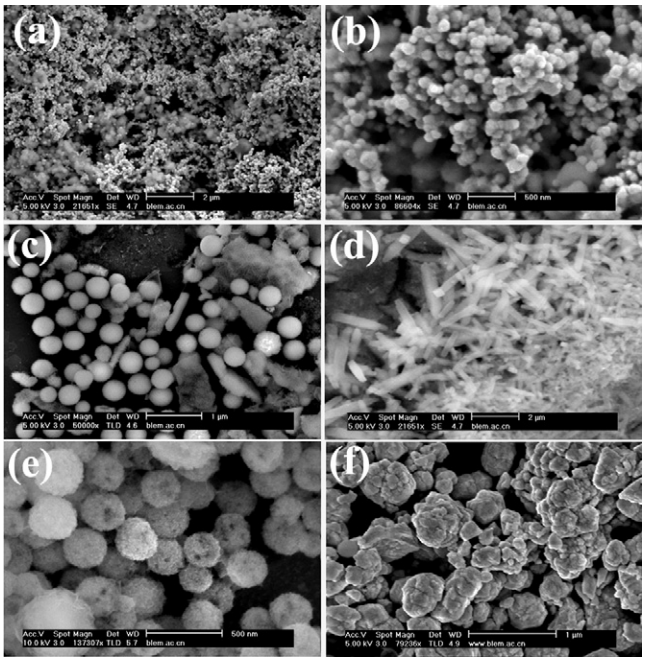

Figure 2. SEM images of two as-synthesized products, showing the variation of morphology when the molar ratio between PVP and $Co(CH_3COO)$ was changed. (a) nPVP/nCo$(CH_3COO) = 12$ and (b) is the enlarged image of (a); (c) nPVP/nCo$(CH_3COO) = 6$; (d) nPVP/nCo$(CH_3COO) = 3$; (e) nPVP/nCo$(CH_3COO) = 1.5$; (f) nPVP/nCo$(CH_3COO) = 0.6$.

insight into the particle size and detailed microstrain involving local lattice distortions [21, 22]. After subtracting the instrumental contribution to line broadening calculated from the diffraction pattern of the instrumental standard silicon (Si) sample, assuming that the particle size (D) and microstrain (ε) contributions to line broadening are independent of each other, the observed line breadth (β) (i.e., the ratio of peak area and height) of the diffraction peaks is simply the sum of the two i.e. $\beta\cos\theta = 0.9\lambda/D + 4\varepsilon\sin\theta$, where 0.9 and λ denote the Scherrer constant and x-ray wavelength, respectively. Plotting the value of $\beta\cos\theta$ as a function of $4\sin\theta$ from the analysis of the XRD diffraction peaks of Co hollow nano-spheres, the microstrain ε can be estimated as 0.018 from the slope of the line and the particle size as 5.5 nm from the intercept with the vertical axis (see footnote 2). The value of the average particle size obtained from the Williamson–Hall method is in agreement with the deduction of the HRTEM analysis that the shell is a system of smaller Co cluster aggregates. Meanwhile, the small Co clusters are not perfectly crystalline but possess grain-interior dislocations and grain-boundary dislocations. Quantitative elemental energy dispersive x-ray (EDX) and inductively couple plasma-atomic emission spectrometry (ICP-AES) analyses show that the hollow structure is Co-rich (see footnote 2). In the PVP stabilized hollow structures, PVP takes about 50%–58.6% of the product weight, and the molar ratio of Co/Pd is 621:1, less than the initial molar ratio of Co/Pd at 1204:1. This indicates that the Co in the reaction mixture is not completely incorporated into the hollow structure. The rest of the Co was found suspended in solution as ICP-AES analysis of the supernatant solution shows a Co concentration of 1.7 μg ml^{-1}.

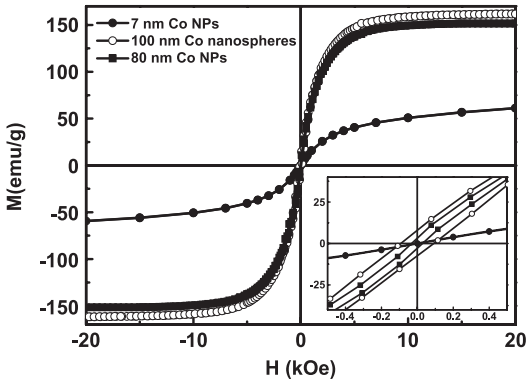

Figure 3. The hysteresis loop of 7 nm, 80 nm Co nano-particles, and 100 nm hollow cobalt materials, measured at 300 K. The inset is the enlarged part at a low magnetic field.

The core dimensions of the hollow spheres can be tuned by controlling the amount of Pd seeds. For example, if the initial concentration of $PdCl_2$ is increased by ten times, the diameter of the hollow cores is reduced from ~200 to ~100 nm. It is evident that an increase in the number of Pd seeds results in a decrease in the average amount of Co available for the shell growth, leading to a smaller core.

The formation of the hollow structure depends strongly on the molar ratio of the repeating amide unit in PVP and $Co(CH_3COO)_2$. If this ratio was larger than 1.5 or smaller than 1, no hollow Co materials were produced, instead various solid cobalt particles were separated. Figure 2(a) shows the SEM image of the solid Co particles synthesized using a procedure similar to the synthesis of hollow Co described above except that the molar ratio of the amide over Co was 12. Figure 2(b) is the enlarged image of a part of figure 2(a). In this case, 90–120 nm solid cobalt particles were synthesized. As the molar ratio of the amide over Co decreased to 6, big solid cobalt particles with a small amount of nano-rods can be observed in the figure 2(c). Figure 2(d) is an SEM image of the product obtained from the amide/Co ratio of 3. It can be seen that under this molar ratio, solid Co particles develop certain rod-like shapes. Figure 2(e) presents an SEM image of the porous Co spheres prepared under the amide/Co ratio of 1.5. When this ratio was further reduced to 0.6, an aggregated cobalt structure was observed, as shown in figure 2(f). These results suggest that under the synthetic conditions reported here, the morphology of the Co particle materials can be readily tuned and the hollow structures are formed only when the amide unit in PVP over $Co(CH_3COO)_2$ falls in the range of 1.0–1.5.

The average molecular weight of PVP can also be used to regulate the morphology of the materials. Under current reaction condition, the use of PVP with an average molecular weight (M_w) above 40 000 is essential for the formation of hollow structured Co. If the M_w of the PVP was 29 000 or 10 000, no hollow Co spheres could be prepared. Instead, the synthesis yielded uncontrolled solid Co aggregates.

Figure 3 shows the room temperature hysteresis loops of the 100 nm hollow Co nano-spheres, 7 and 80 nm Co nano-particles. Herein, 80 nm Co nano-particles are used to compare with 100 nm hollow nano-spheres due to the

consideration of the hollow core. It shows that the porous material is ferromagnetic at room temperature with a coercivity field of 20 Oe (H_c) and a saturation magnetization (M_s) reaching 150 emu g^{-1}, slightly less than the bulk Co value of 163 emu g^{-1} at room temperature, indicating that the Co in the porous structure is mostly metallic. Obviously, it shows a different magnetic behavior comparing with the magnetic properties of the 7 nm Co nano-particles prepared by thermal decomposition or other methods [23–26]. The H_c and M_s at room temperature of 7 nm Co nano-particles with weak or moderately strong dipolar interfacing are zero and about 60 emu g^{-1}, respectively. The increase of H_c and M_s could possibly be attributed to two factors. One is that larger clusters with a size of more than 10 nm existed in the hollow Co nano-spheres, which showed weak ferromagnetic behavior including a small H_c and a slightly high M_s at room temperature. The other is that extremely strong dipolar interactions from the tight packing of superparamagnetic small Co clusters with a size of 1–7 nm in the nano-spheres, made several adjacent Co single-domain clusters have the same orientation of their magnetic moments. This is supported by a lot of research work on the dipolar interaction effect in different magnetic nano-particle systems including Fe, Co, and iron oxides [24, 25]. Meanwhile, the magnetic properties of such a Co nano-sphere system with big aggregate clusters and strong dipolar interaction in small clusters are also different to those of 80 nm Co nano-particles containing atomic moments, whose H_c and M_s are 100 Oe and 163 emu g^{-1}, close to the value of bulk cobalt. This supports the observation result of the HRTEM image that the shell is not single crystalline Co but a system of smaller Co cluster aggregates.

From our experimental observations, we know that the hollow structure can be formed when the Pd nano-particles are present; the average molecular weight of PVP should be over 40 000, and the molar ratio of the amide unit in PVP over Co should be in the range of 1.0–1.5. Using EDX analyses to track the composition change during the reaction, we noticed that the Co/Pd ratio increased with the reaction time. This indicates that Pd nano-particles act as the seeds and PVP regulates the growth of the Co over the seeds during the synthesis. The fact that no Pd peak is found in the x-ray diffraction pattern of the final product (see footnote 2)—indicates that Pd diffuses into the shell matrix of Co. Moreover, a heavy or extremely low coverage of PVP on the surfaces of large cobalt nano-particles might result in an isotropic growth for all different faces. In this regard, the concentration of PVP during the initial stage seems to play an important role in determining the morphologies of the final products. The sizes of the Pd seeds show a broad distribution from 1 to 5 nm as shown in figure 4(a). The Pd seeds can decrease the nucleation energy of Co and thus the Co atoms gradually reduced by EG favor growth on the Pd seeds. At the same time, the amide units in PVP attach to the Co nano-particles and form a big cluster due to the curl of organic chain. Before the final formation of hollow Co nano-spheres, a big cluster with a somewhat fine channel can be clearly observed in the TEM images shown in figure 4(b). With the reaction time increasing, the channel disappears and the hollow nano-spheres form. The schematic illustration of the experimental procedure that generates hollow cobalt nano-spheres by the Pd-seeded polyol process is shown in figure 4(c). Work on elucidation of the mechanism for the formation of hollow Co nano-spheres, such as the very narrow range of the molar ratio of the amide unit in PVP over Co, is still underway.

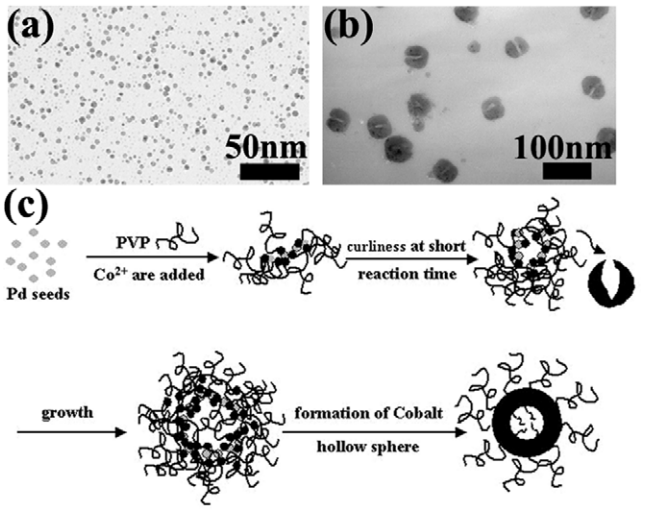

Figure 4. TEM images of (a) Pd seeds and (b) the product synthesized at a reaction time of 5 min. (c) Schematic illustration of the experimental procedure that generates hollow cobalt nano-spheres by the Pd-seeded polyol process.

4. Conclusions

The current synthesis offers a facile way for producing nano-scale magnetic hollow spheres/hemispheres of Co with a tunable core and high magnetic moment. The morphologies of Co materials have a strong dependence on the molar ratio of the amide unit in PVP over Co. A possible formation mechanism of such hollow nano-spheres is useful to find new ways to fabricate different artificial nano-structure materials. All the reagents used are commonly friendly to the environment and the hydrophilic Co nano-spheres/hemispheres are compatible with biomedical molecules. Structures of hollow Co are interesting for molecule storage studies and should have great potential as nano-reactors or nano-capturers for applications in catalysis and magnetic-based separation and delivery.

Acknowledgments

The work was supported by the National Science Foundation of China (Grant No. 90101025), the Science Foundation for Outstanding Young Scientists of China (Grant No. 60328102), and the National '973' Project of China.

References

[1] Tanev P T, Chibwe M and Pinnavaia T J 1994 *Nature* **368** 321
[2] Wijnhoven J E and Vos W L 1998 *Science* **281** 802–4
[3] Barton T J *et al* 1999 *Chem. Mater.* **11** 2633
[4] Caruso F, Caruso R A and Möhwald H 1998 *Science* **282** 1111

[5] Johnson S A, Ollivier P J and Mallouk T E 1999 *Science* **283** 963
[6] Velev O D, Tessier P M, Lenhoff A M and Kaler E W 1999 *Nature* **401** 548
[7] Zhong Z, Yin Y, Gates B and Xia Y 2000 *Adv. Mater.* **12** 206
[8] Landskron K and Ozin G A 2004 *Science* **306** 1529
[9] Huo Q, Margolese D I, Ciesla U, Feng P, Gier T E, Sieger P, Leon R, Petroff P M, Schüth F and Stucky G D 1994 *Nature* **368** 317
[10] Tanev P T and Pinnavaia T J 1995 *Science* **267** 865
[11] Zhao D, Yang P, Chmelka B F and Stucky G D 1999 *Chem. Mater.* **11** 1174
[12] Erlebacher J, Aziz M J, Karma A, Dimitrov N and Sieradzki K 2001 *Nature* **410** 450
[13] Ding Y, Kim Y J and Erlebacher J 2004 *Adv. Mater.* **16** 1897
[14] Yin Y, Rioux R M, Erdonmez C K, Hughes S, Somorjai G A and Alivisatos A P 2004 *Science* **304** 711
[15] Jiang P, Cizeron J, Bertone J F and Colvin V L 1999 *J. Am. Chem. Soc.* **121** 7957
[16] Atwater J E, Akse J R, Jovanovic G N, Wheeler R R Jr and Sornchamni T 2003 *Mater. Res. Bull.* **38** 395
[17] Fiévet F, Lagier J P and Figlarz M 1989 *MRS Bull.* **14** 29
[18] Toneguzzo P, Viau G, Acher O, Fiévet-Vincent F and Fiévet F 1998 *Adv. Mater.* **10** 1031
[19] Sun Y and Xia Y 2002 *Science* **298** 2176
[20] Sun Y, Gates B, Mayers B and Xia Y 2002 *Nano Lett.* **2** 165
[21] Schafler E and Zehetbauer M 2005 *Rev. Adv. Mater. Sci.* **10** 28
[22] Beigmohamadi M, Niyamakom P, Farahzadi A, Kremers S, Michely T and Wuttig M 2008 *Phys. Status Solidi* **2** 1
[23] Yang H T, Shen C M, Su Y K, Yang T Z, Gao H J and Wang Y G 2003 *Appl. Phys. Lett.* **82** 4729
[24] Parker D, Lisiecki I, Salzemann C and Pileni M P 2007 *J. Phys. Chem.* C **111** 12632
[25] Farrell D, Cheng Y H, McCallum R W, Sachan M and Majetich S A 2005 *J. Phys. Chem.* B **109** 13409
[26] Puntes V F, Gorostiza P, Aruguete D M, Bastus N G and Alivisatos A P 2003 *Nat. Mater.* **3** 263